A Half-Size Singularity Test Matrix for Fast and Reliable Passivity Assessment of Rational Models

Adam Semlyen, *Life Fellow, IEEE*, and Bjørn Gustavsen, *Senior Member, IEEE*

***Abstract*—One major difficulty in the rational modeling of linear systems is that the obtained model can be nonpassive, thereby leading to unstable simulations. The model's passivity properties are usually assessed by computing the eigenvalues of a Hamiltonian matrix, which is derived from the model parameters. The purely imaginary eigenvalues represent crossover frequencies where the model's conductance matrix is singular, allowing to pinpoint frequency intervals of passivity violations. Unfortunately, the eigenvalue computation time can be excessive for large models. Also, the test applies only to symmetrical models, and the testing is made difficult by numerical noise in the extracted eigenvalues. In this paper a new (non-Hamiltonian) half-size singularity test matrix is derived for use with admittance parameter state-space models, which overcomes these shortcomings. It gives a computational speedup by a factor of eight; it is applicable to both symmetric and unsymmetrical models; and it produces noiseless eigenvalues for reliable passivity assessment.**

***Index Terms*—Admittance parameters, Hamiltonian matrix, macromodel, passivity, passivity checking, passivity enforcement, rational model, singularity test matrix, state-space model.**

I. Introduction

FREQUENCY-DEPENDENT modeling of linear devices and systems is widely applied in the technical fields of power systems, microwave systems, and high-speed electronic systems. The modeling involves the approximation of characteristic responses in either the frequency domain or the time domain. The end result is a model based on rational functions, thereby allowing efficient time domain simulations by classical discretization methods or recursive convolution [1]. Although it is easy to obtain a quite accurate model having stable poles only (e.g., by using vector fitting [2] with recent advancements [3]–[8]), the obtained model may still result in an unstable simulation. The stability problem is related to passivity violations (i.e., the model generates energy).

The problem of nonpassive models can be mitigated by subjecting the model to a passivity enforcement procedure, where the model parameters are perturbed in a postprocessing step [9]–[14]. These approaches require to assess the model's passivity (i.e., to decide if the model is nonpassive and to characterize the violation). In the frequency domain, the passivity characteristics of admittance parameter models are easily assessed by sweeping along frequency for the eigenvalues of the terminal conductance matrix $\mathbf{G}(\omega)$, since negative eigenvalues imply passivity violations [9], [15]. This approach has the drawback that passivity violations can be missed since the violations can occur between two frequency samples. It has therefore become accepted practice to assess passivity via a particular Hamiltonian matrix, which is calculated directly from the parameters of the rational model [10], [11]. In principle, this permits exact calculation of all frequencies where an eigenvalue of $\mathbf{G}(\omega)$ changes sign, without the need for sweeping.

A disadvantage of this Hamiltonian approach is that the time needed for computing the eigenvalues can be excessive in the case of large models. It has therefore been proposed to save time by calculating only the (few) purely imaginary eigenvalues via a multishift restarted Arnoldi process [16], [17], but a reliable implementation remains a difficult task. A second disadvantage of the Hamiltonian matrix approach is that it only applies to models that are symmetrical (e.g., a pole-residue model), while in reality one also needs to assess passivity for (slightly) unsymmetrical models, for instance models obtained by fitting columns of a terminal admittance matrix $\mathbf{Y}(\omega)$. A third disadvantage is that eigenvalues corresponding to crossover frequencies are not exactly imaginary as they are associated with a small real part (noise). In practice, this requires to use a threshold approach to capture all potential crossover frequencies, followed by a final verification using $\mathbf{G}(\omega)$.

Since the passivity assessment using the Hamiltonian approach can dominate the total computation time for a passivity enforcement procedure, there is a strong need for improving the computational efficiency. There is also a need for extending its applicability to unsymmetrical models, and to avoid the noise problem in the real part of the eigenvalues. A solution to all these issues is provided in this paper.

The paper is organized as follows. Section II reviews the existing approaches for passivity assessment: sweeping and Hamiltonian matrix eigenvalues. Section III derives a new matrix for passivity assessment, starting from the passivity criterion associated with the conductance matrix. The proposed *singularity test matrix* $\mathbf{S}$ has only half the size of the Hamiltonian, and no assumption of symmetry is made. Section IV shows the relation between $\mathbf{S}$ and the traditional Hamiltonian matrix. Sections V through VII compare the performance of the new method with the Hamiltonian approach for some practical

Manuscript received September 27, 2007; revised December 17, 2007. First published May 07, 2008; current version published December 24, 2008. This work was supported in part by the Norwegian Research Council (PETROMAKS Programme), in part by Compagnie Deutsch, in part by FMC Technologies, in part by Framo, in part by Norsk Hydro, in part by Siemens, in part by Statoil, in part by Total, and by Vetco Gray. Paper no. TPWRD-00565-2007.

A. Semlyen is with the Department of Electrical and Computer Engineering, University of Toronto, Toronto, ON M5S 3G4 Canada (e-mail: adam.semlyen@utoronto.ca).

B. Gustavsen is with SINTEF Energy Research, Trondheim N-7465, Norway (e-mail: bjorn.gustavsen@sintef.no).

Color versions of one or more of the figures in this paper are available online at http://ieeexplore.ieee.org.

Digital Object Identifier 10.1109/TPWRD.2008.923406

examples, focusing on computational speed, the implications of model asymmetry, and eigenvalue noise and its implications for passivity assessment.

II. Passivity Assessment

In this section we review some of the main procedures currently in use for passivity assessment. We consider the case of a linear component or system that is characterized by its admittance matrix $\mathbf{Y}$, relating terminal voltages $\mathbf{v}$ and currents $\mathbf{i}$

$$\mathbf{i}(j\omega) = \mathbf{Y}(j\omega)\mathbf{v}(j\omega). \tag{1}$$

The admittance $\mathbf{Y}$ is a symmetric matrix, satisfying the symmetry property (2) and the conjugacy property (3), where the bar indicates conjugate

$$\mathbf{Y} = \mathbf{Y}^T \tag{2}$$

$$\mathbf{Y}(j\omega) = \overline{\mathbf{Y}(-j\omega)}. \tag{3}$$

It is assumed that a rational model for $\mathbf{Y}$ has been identified which satisfies (2) and (3). This can be easily achieved by fitting the elements of $\mathbf{Y}$ using the pole relocating algorithm known as vector fitting (VF) [2]. This leads to a *pole-residue model* (4) which can be expanded into a model in standard state-space form (5). In order to reduce the computation time of the fitting process, one may also choose to fit the columns of $\mathbf{Y}$ with private pole sets. This *columnwise model* has the same structure as the one obtained via the pole-residue model, but the terminal admittance $\mathbf{Y}(j\omega)$ is slightly unsymmetrical

$$\mathbf{Y}(j\omega) \cong \sum_{m=1}^{N} \frac{\mathbf{R}_m}{j\omega - a_m} + \mathbf{D} \tag{4}$$

$$\mathbf{Y}(j\omega) \cong \mathbf{C}(j\omega\mathbf{I} - \mathbf{A})^{-1}\mathbf{B} + \mathbf{D}. \tag{5}$$

Passivity entails that a component cannot generate power, at whatever terminal conditions. This implies that the eigenvalues of the real part of $\mathbf{Y}$ (conductance $\mathbf{G}$) are positive for all frequencies [15]. The passivity criterion (6) (where $eig(\mathbf{A})$ denotes the array of the eigenvalues of matrix $\mathbf{A}$) is based on the expression of the total real power entering the device at its terminals [9] and can be used for assessing bands of passivity violations by sweeping over discrete frequencies

$$eig\left(\mathrm{Re}\left\{\mathbf{Y}(j\omega)\right\}\right. = eig\left(\mathbf{G}(j\omega)\right) > 0. \tag{6}$$

Strictly speaking, the test (6) applies only for symmetrical models but in this paper it will be also used for characterizing slightly unsymmetrical models.

Passivity can also be assessed directly from the state-space model via the eigenvalues of the Hamiltonian matrix (7) [18]. Any purely imaginary eigenvalue of $\mathbf{M}$ corresponds to a frequency where an eigenvalue of $\mathbf{G}$ crosses zero (i.e., where $\mathbf{G}$ is singular). This enables precise identification of bands of passivity violations, without the need for sweeping. We note that the size of $\mathbf{M}$ is twice that of $\mathbf{A}$

$$\mathbf{M} = \begin{bmatrix} \mathbf{A} - \mathbf{B}(\mathbf{D}+\mathbf{D}^T)^{-1}\mathbf{C} & \mathbf{B}(\mathbf{D}+\mathbf{D}^T)^{-1}\mathbf{B}^T \\ -\mathbf{C}^T(\mathbf{D}+\mathbf{D}^T)^{-1}\mathbf{C} & -\mathbf{A}^T + \mathbf{C}^T(\mathbf{D}+\mathbf{D}^T)^{-1}\mathbf{B}^T \end{bmatrix}. \tag{7}$$

It is remarked that a Hamiltonian matrix $\mathbf{A}$ is any matrix that satisfies the relation

$$\mathbf{K}\mathbf{A} + \mathbf{A}^T\mathbf{K} = \mathbf{0} \tag{8}$$

where

$$\mathbf{K} = \begin{bmatrix} \mathbf{0} & \mathbf{I} \\ -\mathbf{I} & \mathbf{0} \end{bmatrix}. \tag{9}$$

III. Singularity Test Matrix

A. Theory

We consider the state equations

$$j\omega\mathbf{x} = \mathbf{A}\mathbf{x} + \mathbf{B}\mathbf{u} \tag{10a}$$

$$\mathbf{y} = \mathbf{C}\mathbf{x} + \mathbf{D}\mathbf{u}. \tag{10b}$$

$\mathbf{A}$, $\mathbf{B}$, $\mathbf{C}$, and $\mathbf{D}$ are assumed to be real (via a similarity transformation). This is essential for the derivation and computationally convenient as shown in Section III-C. We also note that the symmetry of $\mathbf{Y}$ of (5) has no role in the derivations to be presented, thereby making the result applicable for unsymmetrical models as long as the passivity criterion (6) is sufficiently accurate.

In what follows, we focus analytically on the conductance matrix $\mathbf{G}$:

$$\mathbf{G} = \frac{1}{2}\left(\mathbf{Y}(j\omega) + \mathbf{Y}(-j\omega)\right). \tag{11}$$

For $\mathbf{Y}(-j\omega)$, we have the state equations

$$-j\omega\overline{\mathbf{x}} = \mathbf{A}\overline{\mathbf{x}} + \mathbf{B}\mathbf{u} \tag{12a}$$

$$\overline{\mathbf{y}} = \mathbf{C}\overline{\mathbf{x}} + \mathbf{D}\mathbf{u}. \tag{12b}$$

The real part of the output can be written as

$$\mathbf{g} = \frac{1}{2}(\mathbf{y} + \overline{\mathbf{y}}). \tag{13}$$

Inserting (10b) and (12b) into (13) gives

$$\mathbf{g} = \frac{1}{2}\mathbf{C}(\mathbf{x} + \overline{\mathbf{x}}) + \mathbf{D}\mathbf{u}. \tag{14}$$

$\mathbf{G}$ is singular for inputs $\mathbf{u}$ in (14) that make $\mathbf{g} = \mathbf{G}\mathbf{u} = \mathbf{0}$. Such an input $\mathbf{u}$ corresponds to the (real) eigenvector of $\mathbf{G}$ associated with its zero eigenvalue. This gives

$$\mathbf{u} = -\frac{1}{2}\mathbf{D}^{-1}\mathbf{C}(\mathbf{x} + \overline{\mathbf{x}}). \tag{15}$$

Inserting (15) into (10a) gives

$$j\omega\mathbf{x} = \mathbf{A}\mathbf{x} - \frac{1}{2}\mathbf{F}(\mathbf{x}+\overline{\mathbf{x}}) \tag{16}$$

where

$$\mathbf{F} = \mathbf{B}\mathbf{D}^{-1}\mathbf{C}. \tag{17}$$

We next split $\mathbf{x}$ into its real and complex part

$$\mathbf{x} = \mathbf{x}' + j\mathbf{x}'' \tag{18}$$

which gives (16)

$$j\omega(\mathbf{x}' + j\mathbf{x}'') = \mathbf{A}(\mathbf{x}' + j\mathbf{x}'') - \mathbf{F}\mathbf{x}'. \tag{19}$$

For the real and imaginary parts of (19), we get

$$-\omega\mathbf{x}' + \mathbf{A}\mathbf{x}'' = \mathbf{0} \tag{20a}$$
$$(\mathbf{F}-\mathbf{A})\mathbf{x}' - \omega\mathbf{x}'' = \mathbf{0}. \tag{20b}$$

Eliminating either $\mathbf{x}''$ or $\mathbf{x}'$ from (20) gives the eigenvalue problems

$$\left[\mathbf{A}(\mathbf{F}-\mathbf{A}) - \omega^2\mathbf{I}\right]\mathbf{x}' = \mathbf{0} \tag{21a}$$
$$\left[(\mathbf{F}-\mathbf{A})\mathbf{A} - \omega^2\mathbf{I}\right]\mathbf{x}'' = \mathbf{0}. \tag{21b}$$

In (21), ω^2 is the eigenvalue while $\mathbf{x}'$ and $\mathbf{x}''$ are the right eigenvectors of the respective eigenvalue problems (21a) and (21b). From this, it follows that the frequencies ω that produce a singular $\mathbf{G}$ can be calculated as the positive square root of the (positive real) eigenvalues of either matrix $\mathbf{S}$ and $\mathbf{T}$

$$\mathbf{S} = \mathbf{A}(\mathbf{F}-\mathbf{A}) \tag{22a}$$
$$\mathbf{T} = (\mathbf{F}-\mathbf{A})\mathbf{A}. \tag{22b}$$

The purely real elements in the set of ω directly correspond to the crossover frequencies of the eigenvalues of $\mathbf{G}$. In the remainder of this study, we will be assessing passivity using $\mathbf{S}$, which we will call the *singularity matrix*. [Note that the eigenvalues of $\mathbf{S}$ and $\mathbf{T}$ are identical, since for any two unsymmetrical complex square matrices $\mathbf{A}$ and $\mathbf{B}$ are of equal dimension, we have $eig(\mathbf{AB}) = eig(\mathbf{BA})$ [19]. Here, the proof of this is simply that each equation in (21) contains the same eigenvalues as (20)]. After inserting $\mathbf{F}$ from (17), we obtain the detailed result

$$\mathbf{S} = \mathbf{A}(\mathbf{B}\mathbf{D}^{-1}\mathbf{C} - \mathbf{A}) \tag{23a}$$
$$\mathbf{T} = (\mathbf{B}\mathbf{D}^{-1}\mathbf{C} - \mathbf{A})\mathbf{A}. \tag{23b}$$

Theorem: The singularity test matrix $\boldsymbol{S}$ gives, via the subset of its positive-real eigenvalues ω^2, the frequencies ω where $\boldsymbol{G}$ becomes singular and these are the boundaries of passivity violations.

B. Relation Between the Singularity Matrix and Zeros of G

In this section, we show that the eigenvalues of the singularity matrix $\mathbf{S}$ are equal to the zeros of $\mathbf{G}(\omega)$.

The state (10a) can be written as

$$j\omega(\mathbf{x}' + j\mathbf{x}'') = \mathbf{A}(\mathbf{x}' + j\mathbf{x}'') + \mathbf{B}\mathbf{u}. \tag{24}$$

Taking the real and imaginary part of (24) gives

$$\omega\mathbf{x}'' + \mathbf{A}\mathbf{x}' = -\mathbf{B}\mathbf{u} \tag{25a}$$
$$\omega\mathbf{x}' = \mathbf{A}\mathbf{x}''. \tag{25b}$$

Substituting $\mathbf{A}\mathbf{x}''$ from (25b) into (25a) (which has been premultiplied by $\mathbf{A}$) gives, together with (14)

$$(\mathbf{A}^2 + \omega^2\mathbf{I})\mathbf{x}' = -\mathbf{A}\mathbf{B}\mathbf{u} \tag{26a}$$
$$\mathbf{g} = \mathbf{C}\mathbf{x}' + \mathbf{D}\mathbf{u}. \tag{26b}$$

Solving (26a) for $\mathbf{x}'$ and substituting into (26b) gives

$$\mathbf{g} = \left(\mathbf{D} - \mathbf{C}(\mathbf{A}^2 + \omega^2\mathbf{I})^{-1}\mathbf{A}\mathbf{B}\right)\mathbf{u}. \tag{27}$$

This shows that the conductance matrix is

$$\mathbf{G} = \mathbf{D} - \mathbf{C}(\mathbf{A}^2 + \omega^2\mathbf{I})^{-1}\mathbf{A}\mathbf{B} \tag{28}$$

which is of a remarkably simple closed form.

Interchanging in (26) input $\mathbf{u}$ and output $\mathbf{g}$ gives

$$\left(\mathbf{A}(\mathbf{F}-\mathbf{A}) - \omega^2\mathbf{I}\right)\mathbf{x}' = \mathbf{A}\mathbf{B}\mathbf{D}^{-1}\mathbf{g} \tag{29a}$$
$$\mathbf{u} = -\mathbf{D}^{-1}\mathbf{C}\mathbf{x}' + \mathbf{D}^{-1}\mathbf{g} \tag{29b}$$

where we have again introduced (17).

Solving (29a) for $\mathbf{x}'$ and substituting into (29b) we get, noting that $\mathbf{u} = \mathbf{G}^{-1}\mathbf{g}$

$$\mathbf{G}^{-1} = \mathbf{D}^{-1} - \mathbf{D}^{-1}\mathbf{C}\left(\mathbf{A}(\mathbf{F}-\mathbf{A}) - \omega^2\mathbf{I}\right)^{-1}\mathbf{A}\mathbf{B}\mathbf{D}^{-1}. \tag{30}$$

The inspection of (30) shows that the poles of $\mathbf{G}^{-1}$ are given by the "kernel" $\mathbf{A}(\mathbf{F}-\mathbf{A})$, which is precisely the singularity matrix $\mathbf{S}$ of (22a). Consequently, the singularity matrix $\mathbf{S}$ of (22a) gives the zeros of $\mathbf{G}$.

C. Implementation Issues

As mentioned before, it is desirable to have the state-space model converted into a real form (via a similarity transformation; see Appendix). This has the following advantages for an implementation in Matlab [20].

1) With a real $\mathbf{S}$, the eigenvalue computation is substantially faster than for a complex $\mathbf{S}$. In Matlab, the speedup is by a factor of four.
2) With a real $\mathbf{S}$, the eigenvalues corresponding to crossover frequencies of $\mathbf{G}(\omega)$ are purely real. With a complex $\mathbf{S}$, they would be associated with numerical noise in the imaginary part.

IV. Relation With the Hamiltonian Matrix

In order to see the relation with the traditional Hamiltonian matrix $\mathbf{M}$ (7), we also consider the state equation (12a) for $\mathbf{Y}(-j\omega)$. Substituting (15) into (12a) gives

$$-j\omega\overline{\mathbf{x}} = \mathbf{A}\overline{\mathbf{x}} - \frac{1}{2}\mathbf{F}(\mathbf{x}+\overline{\mathbf{x}}). \tag{31}$$

Equation (31) is a homogenous equation in $\mathbf{x}$ and $\overline{\mathbf{x}}$, similarly as (16). These two equations (16) and (31) define the eigenvalue problem

$$\begin{bmatrix} \mathbf{A} - \frac{1}{2}\mathbf{F} - j\omega\mathbf{I} & \frac{1}{2}\mathbf{F} \\ -\frac{1}{2}\mathbf{F} & -\mathbf{A} + \frac{1}{2}\mathbf{F} - j\omega\mathbf{I} \end{bmatrix} \begin{bmatrix} \mathbf{x} \\ -\overline{\mathbf{x}} \end{bmatrix} = \begin{bmatrix} \mathbf{0} \\ \mathbf{0} \end{bmatrix}. \tag{32}$$

This defines the double-size Hamiltonian matrix

$$\tilde{\mathbf{M}} = \begin{bmatrix} \mathbf{A} - \frac{1}{2}\mathbf{F} & \frac{1}{2}\mathbf{F} \\ -\frac{1}{2}\mathbf{F} & -\mathbf{A} + \frac{1}{2}\mathbf{F} \end{bmatrix}. \tag{33}$$

Note that inserting (17) for $\mathbf{F}$ gives exactly $\mathbf{M}$ of (7), when the additional, not generally warranted, assumption $\mathbf{C} = \mathbf{B}^T$ is made. The same eigenvalues are, of course, also obtained with $\mathbf{C} \neq \mathbf{B}^T$, provided that the state space model defines a symmetrical $\mathbf{Y}(\omega)$ of appropriate state space realization. Therefore, usage of $\mathbf{M}$ is only valid for symmetrical models, unlike $\tilde{\mathbf{M}}$ in (33) and the half-size $\mathbf{S}$ in (23a).

Equation (31) is just the conjugate of (16) and therefore it represents redundant information. Indeed, the real and imaginary parts of the two are the same. Therefore, in (32), the eigenvalues $j\omega$ of $\tilde{\mathbf{M}}$ from (33) come in pairs that are not independent. For any positive real ω, we also get its counterpart which is negative real and in which we are not interested. Therefore, it is sufficient to use only (16) and not (31), as we have done before.

V. Example: Pole-Residue Modeling

This example considers the wide-band modeling of a 250-MVA power transformer from a measured admittance matrix. The measurements were made with respect to two of the windings, thereby leading to a 6×6 $\mathbf{Y}(\omega)$ [21].

The admittance matrix was fitted by 160 pole-residue terms, using VF [2] with relaxation [5]. The pole-residue model was expanded into a state-space-model with an A-matrix of dimension 960×960. The rational approximation of $\mathbf{Y}(\omega)$ is shown in Fig. 1 (36 matrix elements).

Using the eigenvalues of $\mathbf{S}$, seven crossover frequencies were detected for the six eigenvalues of $\mathbf{G}(\omega)$, see the left column in Fig. 2. The same frequencies are found in the imaginary part of $\mathbf{M}$ (right column) but they appear two times and they are associated with a small real part. In this case, the presence of a small real part is of no consequence as the eigenvalue can be safely deemed as purely imaginary. However, the double dimension of $\mathbf{M}$ makes the eigenvalue computation about eight times slower, needing as much as 66.6 s (Table I).

In Figs. 3 and 4 (expanded view), the calculated crossover frequencies from $\mathbf{S}$ are shown by stars that are superimposed on a plot of the eigenvalues of $\mathbf{G}(\omega)$. It is seen that the crossover frequencies have been correctly identified.

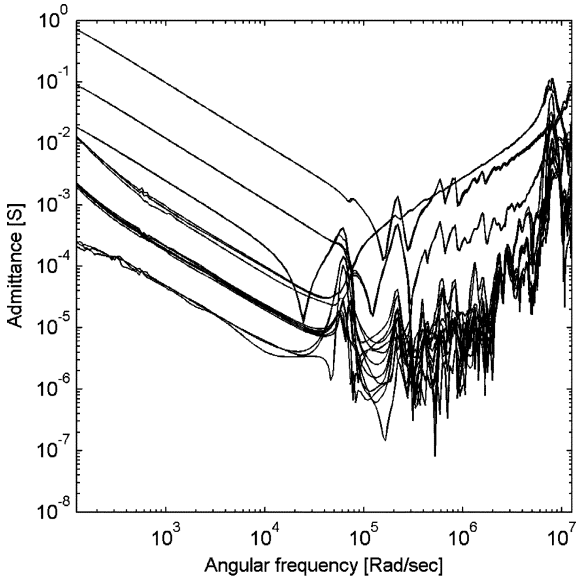

Fig. 1. Frequency response of the rational model.

$\sqrt{eig(\mathbf{S})}$	$eig(\mathbf{M})$
1.6115e+007	5.3551e-009 +1.6115e+007i
1.3863e+007	5.3551e-009 -1.6115e+007i
1.3472e+007	4.7148e-008 +1.3863e+007i
1.3229e+007	4.7148e-008 -1.3863e+007i
1.3170e+007	-5.1223e-009 +1.3472e+007i
1.2857e+007	-5.1223e-009 -1.3472e+007i
1.2832e+007	-1.0664e-007 +1.3229e+007i
	-1.0664e-007 -1.3229e+007i
	7.5554e-008 +1.3170e+007i
	7.5554e-008 -1.3170e+007i
	-5.1223e-009 +1.2857e+007i
	-5.1223e-009 -1.2857e+007i
	-5.5879e-009 +1.2832e+007i
	-5.5879e-009 -1.2832e+007i

Fig. 2. Eigenvalues of $\mathbf{S}$ and $\mathbf{M}$ that correspond to singularities of $\mathbf{G}$.

TABLE I
Time Consumption for Eigenvalue Computation

Matrix	Size	CPU time for diagonalization [sec]
S	960	8.5
M	1920	66.6

VI. Example: Columnwise Modeling

We continue with the example in Section V, but this time, we fit $\mathbf{Y}(\omega)$ with its columns $(N = 140)$, thereby obtaining a model with a private pole set for each column. The structure is identical to the one obtained via pole-residue modeling (see the Appendix), but the model's $\mathbf{Y}$ is now slightly unsymmetrical (eigenvalues not strictly real).

Using $\mathbf{S}$, a total of 21 crossovers were predicted for the eigenvalues of $\mathbf{G}(\omega)$, while $\mathbf{M}$ resulted in 30 crossovers. A careful comparison with the (real part) of $eig(\mathbf{G})$ showed that the result by $\mathbf{M}$ is in error. This is clearly seen in Fig. 5 for a high-frequency portion of the response. Here, a crossover at about $3.75E7$ rad/s is missed out by the assessment using $\mathbf{M}$. Fig. 6

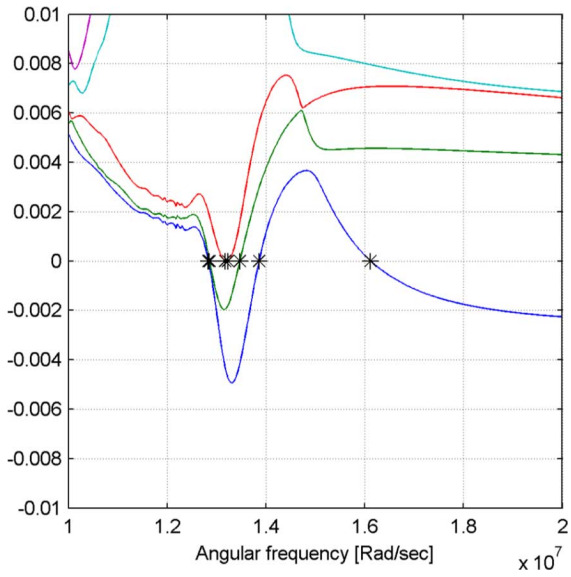

Fig. 3. Eigenvalues of $\mathbf{G}(\omega)$.

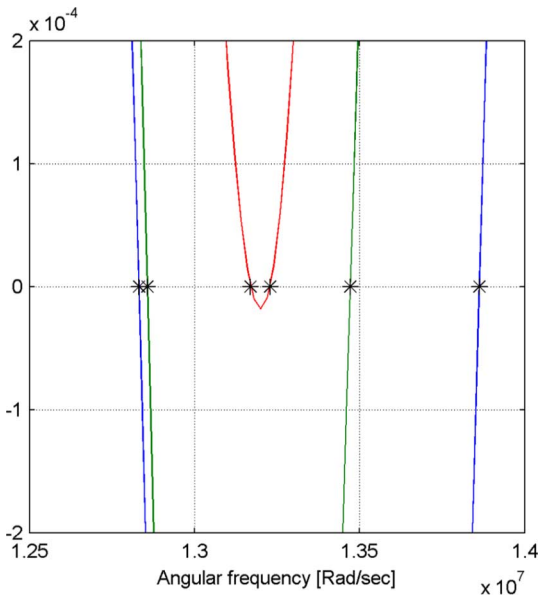

Fig. 4. Eigenvalues of $\mathbf{G}(\omega)$. Expanded view.

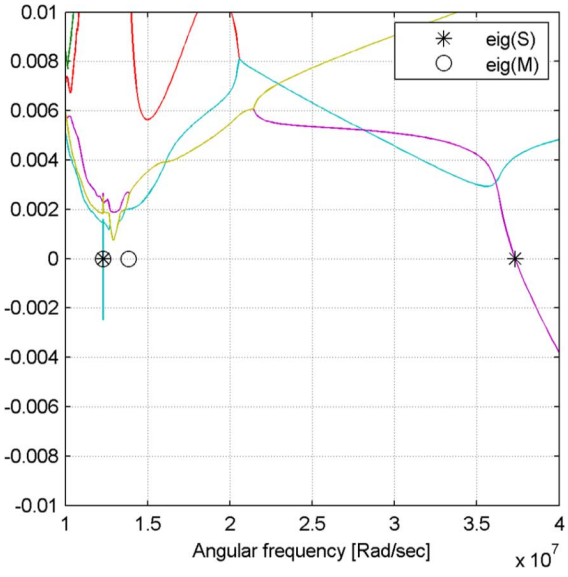

Fig. 5. Real part of eigenvalues of $\mathbf{G}(\omega)$. High-frequency range.

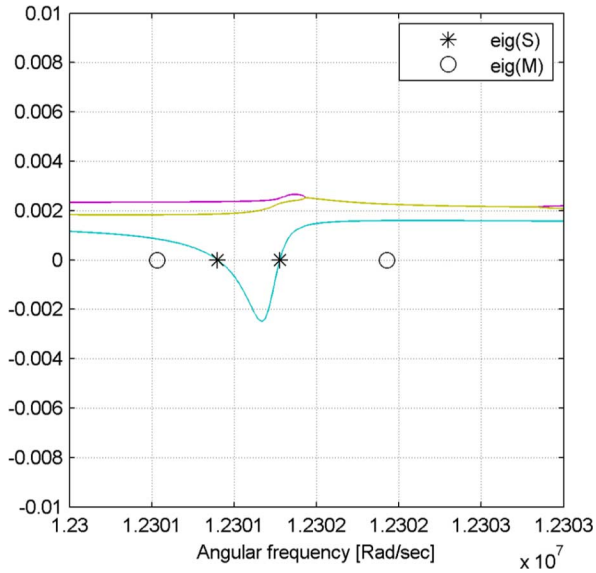

Fig. 6. Real part of eigenvalues of $\mathbf{G}(\omega)$. High-frequency range, expanded view.

shows an expanded view of the local, negative peak around $1.23E7$ rad/s. It is seen that the result obtained using $\mathbf{M}$ is incorrect whereas the usage of $\mathbf{S}$ leads to the correct result.

In the plots, it appears that single eigenvalues become split into two eigenvalues at certain frequencies. This result is due to conjugate pairs that change into two real eigenvalues (the pair of conjugate eigenvalues have identical real parts).

VII. Example: Noise Problem With Hamiltonian Matrix

In this example, we consider the 6×6 terminal admittance matrix $\mathbf{Y}(\omega)$ of a three-phase overhead line, which is subjected to pole-residue modeling by a common pole set. This is the same line configuration as reported in [12].

Fig. 7 shows the eigenvalues of the Hamiltonian matrix $\mathbf{M}$ (7), expressed in the form of the absolute value of the real part divided by the imaginary part. The plot includes only one eigenvalue out of each conjugate pair and only eigenvalues with a ratio smaller than unity are included. Thus, eigenvalues with a very small ratio represent the "purely" imaginary eigenvalues. However, from the plot it can be seen that there is no clear cut-off between the nearly imaginary eigenvalues and the rest. (A threshold value for correct passivity assessment would have to lie in the narrow band between $1E-5$ and $3E-3$.) This makes it difficult to devise a fail-proof passivity assessment test based on $\mathbf{M}$ alone.

On the other hand, usage of $\mathbf{S}$ still leads to purely real eigenvalues for the crossover frequencies of the eigenvalues of $\mathbf{G}$. Figs. 8 and 9 show the eigenvalues of $\mathbf{G}(\omega)$ together with the

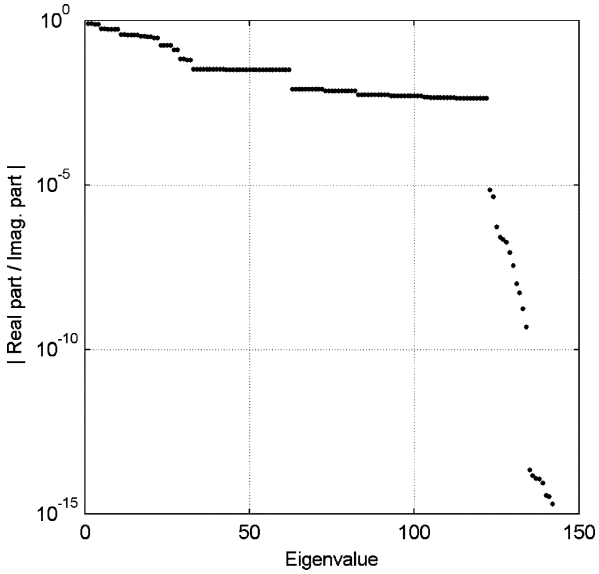

Fig. 7. Eigenvalues of $\mathbf{M}$.

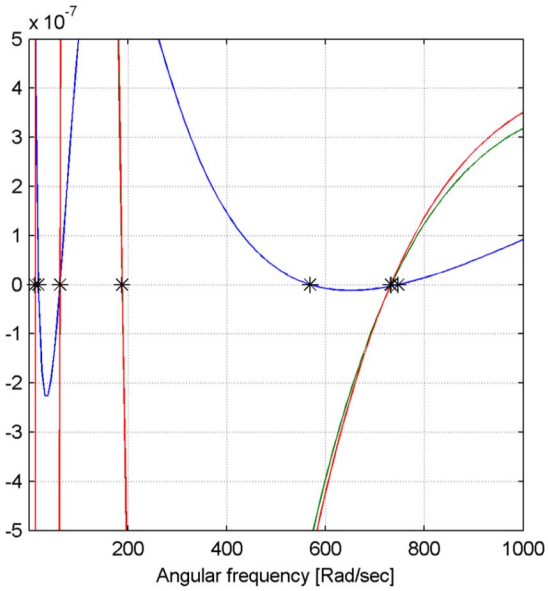

Fig. 8. Eigenvalues of $\mathbf{G}(\omega)$. Low frequency range.

crossover frequencies calculated from $\mathbf{S}$, again verifying the correctness of the approach.

VIII. Discussion

In the case of very large models, the computation of the eigenvalues of $\mathbf{S}$ can still be prohibitively long, since the computation time increases cubically with the size of $\mathbf{S}$. In such situations, the usage of $\mathbf{S}$ could be combined with the procedures in [16] and [17] which reduce computation time by calculating only the (few) eigenvalues of interest.

The singularity test matrix $\mathbf{S}$ can also be applied for models that have been obtained by fitting impedance matrices $\mathbf{Z}(\omega)$, rather than admittance matrices. This follows since the passivity criterion is now that the real part of $\mathbf{Z}(\omega)$ has positive eigenvalues.

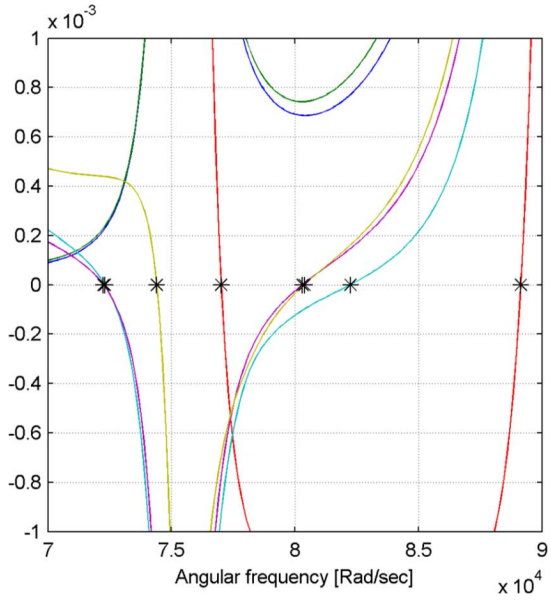

Fig. 9. Eigenvalues of $\mathbf{G}(\omega)$. High frequency range.

IX. Conclusions

This paper has introduced a new (non-Hamiltonian) singularity test matrix for passivity assessment of admittance parameter state-space models.

1) The new test matrix $\mathbf{S}$ identifies via its eigenvalues, the frequencies where the conductance matrix $\mathbf{G}$ is singular. The singularities are also the zeros of $\mathbf{G}$.
2) The square root of purely-real eigenvalues of $\mathbf{S}$ correspond to frequencies where eigenvalues of $\mathbf{G}$ change sign (i.e., boundaries of passivity violations).
3) The computation of eigenvalues is about eight times faster when using $\mathbf{S}$ instead of the traditional Hamiltonian matrix $\mathbf{M}$.
4) The test matrix $\mathbf{S}$ is applicable to both symmetric and unsymmetrical models, unlike $\mathbf{M}$ which only applies to symmetric models.
5) The problem of numerical noise in the real part of the eigenvalues of $\mathbf{M}$ does not exist with $\mathbf{S}$, provided that a real-only state-space model is used.

Appendix
Conversion of Pole-Residue Model to Real-Only State Space Model

As was shown in [22], a pole-residue model (4) can be brought to the form (34) by factorizing each term

$$\mathbf{R}_m \cdot \frac{1}{j\omega - a_m} = \mathbf{R}_m \cdot \left(\frac{1}{j\omega - a_m} \cdot \mathbf{I}_n \right) \cdot \mathbf{I}_n \qquad (34)$$

where $\mathbf{I}_n$ is an identity matrix of the same size as $\mathbf{R}_m$. The building of $\mathbf{A}$, $\mathbf{B}$, $\mathbf{C}$ from each contribution (34) is done as shown in Fig. 10, with $n = 3$ and $N = 4$.

The columns in $\mathbf{C}$ and rows in $\mathbf{B}$ are rearranged to produce the structure in Fig. 11. Each block now represents one column of $\mathbf{Y}$.

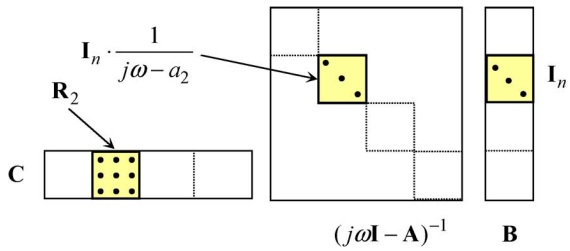

Fig. 10. Contribution from the second term $(m = 2)$ in (4).

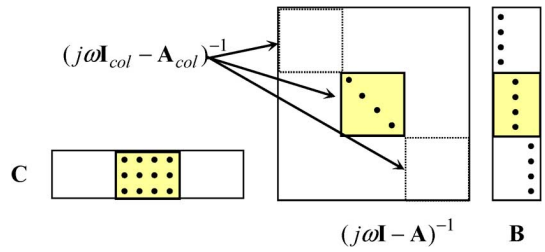

Fig. 11. Columnwise realization.

It is assumed that the poles are arranged so that complex poles appear in conjugate pairs on the diagonal. For each pair, the corresponding submatrices are modified (via a similarity transformation) into a real-only model as follows [23]:

$$\hat{\mathbf{A}} = \begin{bmatrix} \mathrm{Re}\{a\} & \mathrm{Im}\{a\} \\ -\mathrm{Im}\{a\} & \mathrm{Re}\{a\} \end{bmatrix}, \quad \hat{\mathbf{c}} = [\mathrm{Re}\{\mathbf{c}\} \quad \mathrm{Im}\{\mathbf{c}\}] \tag{35}$$

$$\hat{\mathbf{b}} = \begin{bmatrix} 2\mathrm{Re}\{\mathbf{b}^T\} \\ -2\mathrm{Im}\{\mathbf{b}^T\} \end{bmatrix} = \begin{bmatrix} 2\mathbf{b}^T \\ \mathbf{0}^T \end{bmatrix}. \tag{36}$$

The same transformation (35) and (36) also applies when the state-space model has been obtained by columnwise fitting of $\mathbf{Y}$. In that case, however, the state-space model produces a slightly unsymmetrical $\mathbf{Y}$, since a different pole set will be obtained for the different columns.

ACKNOWLEDGMENT

The authors thank M. Tiberg (ABB Sécheron Ltd., Switzerland) for providing the transformer measurements in Sections V and VI.

REFERENCES

[1] A. Semlyen and A. Dabuleanu, "Fast and accurate switching transient calculations on transmission lines with ground return using recursive convolutions," *IEEE Trans. Power App. Syst.*, vol. 94, no. 2, pt. 1, pp. 561–575, Mar./Apr. 1975.

[2] B. Gustavsen and A. Semlyen, "Rational approximation of frequency domain responses by vector fitting," *IEEE Trans. Power Del.*, vol. 14, no. 3, pp. 1052–1061, Jul. 1999.

[3] S. Grivet-Talocia, "Package macromodeling via time-domain vector fitting," *IEEE Microw. Wireless Compon. Lett.*, vol. 13, no. 11, pp. 472–474, Nov. 2003.

[4] S. Grivet-Talocia and M. Bandinu, "Improving the convergence of vector fitting for equivalent circuit extraction from noisy frequency responses," *IEEE Trans. Electromagn. Compat.*, vol. 48, no. 1, pp. 104–120, Feb. 2006.

[5] B. Gustavsen, "Improving the pole relocating properties of vector fitting," *IEEE Trans. Power Del.*, vol. 21, no. 3, pp. 1587–1592, Jul. 2006.

[6] D. Deschrijver, B. Haegeman, and T. Dhaene, "Orthonormal vector fitting: A robust macromodeling tool for rational approximation of frequency domain responses," *IEEE Trans. Adv.Packag.*, vol. 30, no. 2, pp. 216–225, May 2007.

[7] D. Deschrijver, B. Gustavsen, and T. Dhaene, "Advancements in iterative methods for rational approximation in the frequency domain," *IEEE Trans. Power Del.*, vol. 22, no. 3, pp. 1633–1642, Jul. 2007.

[8] B. Gustavsen and C. Heitz, "Rational modeling of multiport systems by modal vector fitting," in *Proc. 11th IEEE Workshop on Signal Propagation on Interconnects*, Genova, Italy, May 13–16, 2007, pp. 49–52, Ruta di Camogli.

[9] B. Gustavsen and A. Semlyen, "Enforcing passivity for admittance matrices approximated by rational functions," *IEEE Trans. Power Syst.*, vol. 16, no. 1, pp. 97–104, Feb. 2001.

[10] D. Saraswat, R. Achar, and M. S. Nakhla, "A fast algorithm and practical considerations for passive macromodeling of measured/simulated data," *IEEE Trans. Adv. Packag.*, vol. 27, no. 1, pp. 57–70, Feb. 2004.

[11] S. Grivet-Talocia, "Passivity enforcement via perturbation of Hamiltonian matrices," *IEEE Trans. Circuits Syst. I*, vol. 51, no. 9, pp. 1755–1769, Sep. 2004.

[12] B. Gustavsen, "Passivity enforcement of rational models via model perturbation," *IEEE Trans. Power Del.*, vol. 23, no. 2, pp. 768–775, Apr. 2008.

[13] B. Gustavsen, "Fast passivity enforcement of rational macromodels by perturbation of residue matrix eigenvalues," in *Proc. 11th IEEE Workshop Signal Propagation on Interconnects*, Genova, Italy, May 13–16, 2007, pp. 71–74.

[14] A. Lamecki and M. Mrozowski, "Equivalent SPICE circuits with guaranteed passivity from nonpassive models," *IEEE Trans. Microw. Theory Tech.*, vol. 55, no. 3, pp. 526–532, Mar. 2007.

[15] S. Boyd and L. O. Chua, "On the passivity criterion for LTI n-ports," *Circuit Theory Appl.*, vol. 10, pp. 323–333, 1982.

[16] S. Grivet-Talocia, "Fast passivity enforcement for large and sparse macromodels," in *Proc. 13th IEEE Topical Meeting Electrical Performance of Electronic Packaging*, Portland, OR, Oct. 25–27, 2004, pp. 247–250.

[17] S. Grivet-Talocia, "An adaptive sampling technique for passivity characterization and enforcement of large interconnect macromodels," *IEEE Trans. Adv. Packag.*, vol. 30, no. 2, pp. 226–237, May 2007.

[18] S. Boyd, L. E. Ghaoui, E. Feron, and V. Balakrishnan, *Linear Matrix Inequalities in System and Control Theory*. Singapore: SIAM, 1994, vol. 15, Studies Appl. Math. [Online]. Available: http://www.stanford.edu/~boyd/lmibook/.

[19] G. H. Golub and C. F. Van Loan, *Matrix Computations*, 2nd ed. Baltimore, MD: Johns Hopkins Univ. Press, p. 340.

[20] The Mathworks, Inc. Natick, MA. [Online]. Available: http://www.mathworks.com.

[21] M. Tiberg, D. Bormann, B. Gustavsen, C. Heitz, O. Hoenecke, G. Muset, J. Mahseredjian, and P. Werle, "Generic and automated simulation modeling based on measurements," in *Proc. Int. Conf. Power Systems Transients*, Lyon, France, Jun. 4–7, 2007, p. 6.

[22] B. Gustavsen and A. Semlyen, "A robust approach for system identification in the frequency domain," *IEEE Trans. Power Del.*, vol. 19, no. 3, pp. 1167–1173, Jul. 2004.

[23] E.-P. Li, E.-X. Liu, L.-W. Li, and M.-S. Leong, "A coupled efficient and systematic full-wave time-domain macromodeling and circuit simulation method for signal integrity analysis of high-speed interconnects," *IEEE Trans. Adv. Packag.*, vol. 27, no. 1, pp. 213–223, Feb. 2004.

Adam Semlyen (LF'97) was born in 1923 in Romania. He received the Dipl. Ing. and Ph.D. degree.

He began his career in Romania with an electric power utility and held academic positions at the Polytechnic Institute of Timisoara. In 1969, he joined the University of Toronto, Toronto, ON, Canada, where he is a Professor in the Department of Electrical and Computer Engineering, emeritus since 1988. His research interests include steady state and dynamic analysis as well as computation of electromagnetic transients in power systems.

Bjørn Gustavsen (M'94–SM'03) was born in Harstad, Norway in 1965. He received the M.Sc. and Dr.Ing. degrees from the Norwegian Institute of Technology (NTH), Trondheim, in 1989 and 1993, respectively.

Since 1994, he has been with SINTEF Energy Research, Trondheim. His interests include simulation of electromagnetic transients and modeling of frequency-dependent effects. He spent 1996 as a Visiting Researcher at the University of Toronto, Toronto, ON, Canada, and the summer of 1998 at the Manitoba HVDC Research Centre, Winnipeg, MB, Canada. He was a Marie Curie Fellow at the University of Stuttgart, Germany, during August 2001–August 2002.